

# Geometric scaling violations in the central rapidity region of d+Au collisions at RHIC

Adrian Dumitru<sup>a</sup>, Arata Hayashigaki<sup>a</sup> and Jamal Jalilian-Marian<sup>b</sup>

*<sup>a</sup>Institut für Theoretische Physik, J. W. Goethe Universität  
Max-von-Laue Strasse 1*

*D-60438 Frankfurt am Main, Germany*

*<sup>b</sup>Institute for Nuclear Theory, University of Washington, Seattle, WA 98195*

## Abstract

We show that geometric scaling is satisfied to good accuracy in the forward region of d+Au collisions at RHIC. Scaling violations do show up, however, at mid-rapidity, and the anomalous dimension of the small- $x$  gluon distribution evolves to near its DGLAP limit for transverse momenta of a few GeV. This represents a first consistency check of RHIC deuteron-nucleus and HERA DIS phenomenology, and of the universality of the underlying Color Glass Condensate (CGC) theory, which describes both phenomena. It also reconciles successful leading-twist LO and NLO perturbative QCD computations of mid-rapidity particle production with small- $x$  evolution. Finally, we introduce a new parameterization for the anomalous dimension of the small- $x$  gluon distribution which properly reproduces known theoretical limits at large rapidity, at large virtuality, and on the saturation boundary, and still fits the available data from d+Au collisions at RHIC. We find indications that sub-asymptotic terms in the rapidity-evolution of the anomalous dimension are large.

# 1 Introduction

The weak-coupling gluon saturation formalism [1, 2] has been used at HERA, rather successfully, in order to describe the  $x$  and  $Q^2$  dependence of the inclusive proton structure function  $F_2(x, Q^2)$ . Specifically, the simple Golec-Biernat and Wüsthoff (GBW) model [3] provided a very efficient qualitative “summary” of the small- $x$ , moderate  $Q^2$  data in terms of an initial condition  $Q_s^2(x_0) = Q_0^2$  for the saturation momentum and its (constant) growth rate  $\lambda = \partial \log Q_s^2 / \partial \log 1/x$ . It led to the discovery of the interesting phenomenon of “geometric scaling” [4], implying that in the relevant range of  $x$  and  $Q^2$ , the structure function depends on  $x$  and  $Q^2$  exclusively via the scaling variable  $Q^2/Q_s^2(x)$ . In other words, that the scattering cross section for a dipole of size  $r_t$  does not depend on  $r_t$  and  $x$  separately but only through the combination  $\rho = r_t Q_s(x)$ .

This phenomenon does not find a natural explanation within the linear Dokshitzer, Gribov, Lipatov, Altarelli, Parisi (DGLAP) [5] and Balitsky, Fadin, Kuraev, Lipatov (BFKL) [6] QCD evolution equations in the absence of saturation boundary conditions. It has been shown to arise from the BFKL equation *with* saturation boundary conditions [7], in an expansion of the LO-BFKL solution to first order about the saturation line, and in mean-field approximation. That equation, with the corresponding boundary condition, represents an approximation to the full non-linear “Color Glass Condensate” (CGC) theory of QCD evolution. It is valid only on one side of the saturation line  $Q_s(x)$ , in the dilute regime.

Moreover, refs. [7] also computed the *scaling violations*<sup>1</sup> which emerge away from the saturation boundary at  $Q^2 \gg Q_s^2(x)$ . They arise from the diffusion term in the expansion of the LO-BFKL solution to second order about the saturation saddle-point, which shifts the anomalous dimension  $\gamma$  of the target gluon distribution by  $\Delta\gamma \sim y^{-1} \log(1/r_t Q_s(y))$  as one moves away from the saturation boundary ( $y = \log 1/x$  denotes rapidity). By  $Q_{gs}^2(x) \sim Q_s^4(x)/\Lambda^2$ , scaling violations grow to order one ( $\Lambda$  is a non-perturbative scale in the infrared, of order  $\Lambda_{\text{QCD}}$ );  $Q_{gs}$  is the upper boundary of the so-called geometric scaling window. Beyond this virtuality, the target gluon distribution is described for example by the DLA form, if  $y$  and  $\log Q^2$  are sufficiently large.

A fit to the HERA data in the (“extended”) geometric scaling window  $Q_s^2(x) < Q^2 < Q_{gs}^2(x)$  has been performed by Iancu, Itakura and Munier (IIM) in ref. [8] (see also [9]), employing a dipole parameterization which represents an approximate solution to the JIMWLK equations [10] governing the mean-field evolution of color dipoles. They find evidence for scaling violations in the HERA data, as predicted by the CGC theory: a substantial increase of  $\gamma$  with  $1/r_t$  is required to improve the agreement with the data as compared to the original GBW dipole model.

In recent years, new data on single-inclusive hadron production at semi-hard transverse momenta emerged from the Relativistic Heavy-Ion Collider (RHIC). Here, we are interested in particular in data from deuteron-gold collisions at central and forward rapidity (toward the fragmentation region of the deuteron projectile) [11, 12, 13, 14], which may probe

---

<sup>1</sup>We shall use this terminology throughout the manuscript to refer to violations of *geometric scaling* away from the saturation line, not to the violation of  $Q^2$  scaling due to DGLAP evolution.

high gluon densities in the gold target, and at the same time, should be less affected by final-state effects than nucleus-nucleus collisions.

A first semi-quantitative analysis of the d+Au data from RHIC was performed by Kharzeev, Kovchegov and Tuchin (KKT) in ref. [15], identifying qualitative features of the expected CGC evolution and providing an alternative dipole parameterization: the KKT model, to be described below, was constructed to fit RHIC instead of HERA data. In ref. [16], we extended the standard CGC approach to particle production to include recoil effects of the large- $x$  projectile partons, and found very good quantitative agreement with RHIC data at large rapidity using either the KKT or the IIM dipole. It turned out that a crucial feature of both dipole models lies in the fact that the target anomalous dimension at large rapidity and moderate  $p_t$  is essentially constant,  $\gamma \approx 0.6$ , and substantially smaller than in the DGLAP regime ( $\gamma_{DGLAP} \sim 1$ ). Hence, for transverse momenta of a few GeV and rapidity  $y_h \gtrsim 3$ , the data points are in either the saturation or extended scaling regions, where scaling violations are essentially *absent* at RHIC energy.

In the present paper, we extend our previous calculation of forward hadron production [16] to the mid-rapidity region. Our main objective is to analyze whether scaling violations, as predicted by the CGC theory and previous dipole fits to HERA data, show up. This is a necessary condition for establishing the CGC as a universal theory of QCD evolution near a saturation boundary within the weak-coupling (semi-hard) regime.

The paper is organized as follows. In the next section, we introduce the formula for the single-inclusive hadron production cross section in high-energy proton (or deuteron) collisions with a heavy nucleus which accounts for both small- $x$  evolution of the dense target and full DGLAP evolution of the dilute projectile. We also present the KKT dipole parameterization there. In section 3 we apply this formalism to hadron production at mid-rapidity and compare to data from RHIC to check for the presence of scaling violations. In section 4 we modify the IIM dipole parameterization, in particular that of the anomalous dimension, to fit the available data from RHIC at central and at forward rapidity, which is done in section 5. Finally, section 6 contains our summary and conclusion.

## 2 Proton-Nucleus Collisions within the CGC approach

The single-inclusive hadron production cross section in p+A collision is given by [16]

$$x_F \frac{d\sigma^{pA \rightarrow hX}}{dx_F d^2p_t d^2b} = \frac{1}{(2\pi)^2} \int_{x_F}^1 dx_p \frac{x_p}{x_F} \left[ f_{q/p}(x_p, Q_f^2) N_F \left( \frac{x_p}{x_F} p_t, b \right) D_{h/q} \left( \frac{x_F}{x_p}, Q_f^2 \right) + f_{g/p}(x_p, Q_f^2) N_A \left( \frac{x_p}{x_F} p_t, b \right) D_{h/g} \left( \frac{x_F}{x_p}, Q_f^2 \right) \right], \quad (1)$$

where  $p_t$  and  $x_F$  are the transverse momentum and the Feynman- $x$  of the produced hadron, respectively.  $x_p$  denotes the momentum fraction of a projectile parton and  $b$  is the impact parameter. Note that this expression is different from the more common  $k_t$  factorized

expressions [6, 17] in that *the radiation vertex is exact*. The common eikonal (soft gluon) approximation made in the  $k_t$ -factorization approach is omitted, which reflects in the fact that the projectile parton distribution functions  $f(x_p, Q_f^2)$ , and their fragmentation functions  $D(z, Q_f^2)$  into hadrons, evolve according to the full DGLAP [5] evolution equations and respect the momentum sum-rule. The importance of this evolution for the interpretation of forward-rapidity data from RHIC is discussed in detail in [16].

Eq. (1) resums large logarithms of  $1/x_A$  arising from evolution of the target wave function with energy as well as logarithms of  $Q^2$  from evolution of the collinearly factorized projectile quark and gluon distributions with  $Q^2$ . It does not include large- $x$  effects such as recoil in the nucleus, nor does it account for logarithms of  $Q^2$  on the target side (only collinear emissions from the projectile are included, c.f. ref. [16] for details). Therefore, this expression is valid when the projectile partons are in either the full or double-log DGLAP kinematics (in other words, above the “extended” geometric scaling window for the projectile) while the target is in the small- $x_A$ , high-density regime.

To illustrate the regime of applicability of eq. (1) from another perspective we compare to the usual  $k_t$ -factorization approach, where the single-inclusive gluon production cross section is given by

$$\frac{d\sigma}{dyd^2p_t} = F \int dk_t^2 \frac{p_t^2}{k_t^2(k_t - p_t)^2} \phi_p(x_p, k_t^2) \phi_A(x_A, (k_t - p_t)^2). \quad (2)$$

The pre-factor  $F = 4\pi\alpha_s N_c / (N_c^2 - 1) / p_t^4$  and  $\phi_{p,A}(x_{p,A}, k_t^2) = \partial x_{p,A} g(x_{p,A}, k_t^2) / (\partial \log k_t^2)$  denote the unintegrated gluon distribution functions of the proton and of the nucleus, respectively.

To leading  $\log p_t^2$  accuracy we only need to pick up the contributions from  $k_t \sim 0$  and  $k_t \sim p_t$ :

$$\frac{1}{F} \frac{d\sigma}{dyd^2p_t} \approx \int_0^{p_t^2} dk_t^2 \frac{1}{k_t^2} \phi_p(x_p, k_t^2) \phi_A(x_A, p_t^2) + \int_0^{p_t^2} dk_t^2 \frac{1}{k_t^2} \phi_p(x_p, p_t^2) \phi_A(x_A, k_t^2) \quad (3)$$

$$= x_p g(x_p, p_t^2) \phi_A(x_A, p_t^2) + \phi_p(x_p, p_t^2) \int_0^{p_t^2} dk_t^2 \frac{1}{k_t^2} \phi_A(x_A, k_t^2). \quad (4)$$

In the second term, we shifted  $(k_t - p_t)^2 \rightarrow k_t^2$ .

The first term corresponds to eq. (1), if one replaces the  $D_{h/g}(z)$  fragmentation function from there by  $\delta(1-z)$  (we are now discussing gluon, not hadron production) and identifies

$$F \phi_A(p_t) = \frac{N_A(p_t)}{(2\pi)^2}. \quad (5)$$

Nevertheless, one should keep in mind that eq. (2) is derived in the recoilless approximation and so is not applicable when  $x_p$  is large, say  $\geq 0.01$  for a proton projectile. As already mentioned above, eq. (1) was derived without this limitation [16].

On the other hand, the second term from (4) is clearly not part of eq. (1). For  $p_t \sim Q_{gs}$  (the geometric scaling momentum of the nucleus) the unintegrated gluon distribution

functions are given by (see e.g. [18])

$$\phi_p(x_p, p_t^2) \sim 1 \quad , \quad \phi_A(x_A, k_t^2) \sim S_A k_t^2 \left( \frac{Q_s^2(x_A)}{k_t^2} \right)^\gamma . \quad (6)$$

Here,  $S_A$  denotes the transverse area of the nucleus and  $\gamma < 1$  is the anomalous dimension of its gluon distribution function, see below. Constant prefactors which are irrelevant for the present discussion have been dropped. Using these expressions in (3) shows that no logarithms of  $p_t^2$  arise from the second term, which therefore is suppressed. On the other hand, for  $p_t \gg Q_{gs}(x_A)$ , the integral over  $k_t^2$  in the second term of (4) *does* give rise to a contribution  $\sim \log(p_t^2/Q_{gs}^2)$  since  $\phi_A(x_A, k_t^2) \sim 1$  for  $k_t > Q_{gs}$ . Hence, for  $p_t \gg Q_{gs}$  collinear emissions from the target have to be included as well, for example by using CCFM unintegrated gluon distributions [19].

The purpose of the present manuscript is to check for the presence of geometric scaling violations in the mid-rapidity data from RHIC. Consequently, we focus on the regime of moderately large transverse momenta not too far above  $Q_{gs}$ . Since there  $x_p \gtrsim 0.01$ , we believe that it is more appropriate to employ eq. (1) rather than (2).

The cross section depends on the scattering probability of dipoles of size  $r_t$  in the fundamental and adjoint representations, respectively, at an impact parameter  $b$ :

$$\begin{aligned} N_F(r_t, b) &\equiv \frac{1}{N_c} \text{Tr}_c \langle 1 - V^\dagger(b - r_t/2) V(b + r_t/2) \rangle, \\ N_A(r_t, b) &\equiv \frac{1}{N_c^2 - 1} \text{Tr}_c \langle 1 - U^\dagger(b - r_t/2) U(b + r_t/2) \rangle, \end{aligned} \quad (7)$$

where  $V$  and  $U$  denote Wilson lines along the light cone [10] in the corresponding representation, and  $N_c$  is the number of colors.

In practice, the ab-initio determination of dipole profiles by solution of the JIMWLK equations is not feasible yet. Therefore, one resorts to theory-motivated phenomenological parametrizations of the dipole profile which can be tested against data. An example is the KKT model [15], where the dipole profile is parameterized as

$$N_A(r_t, y_h) = 1 - \exp \left[ -\frac{1}{4} (r_t^2 Q_s^2(y_h))^{\gamma(y_h, r_t)} \right], \quad (8)$$

with  $y_h$  the rapidity of the produced hadron. The saturation scale of the nucleus at  $y_h$  is given as<sup>2</sup>

$$Q_s(y_h) = Q_0 \exp[\lambda(y_h - y_0)/2]. \quad (9)$$

Here,  $\lambda \simeq 0.3$  is fixed by the DIS data and the initial condition  $Q_0 \simeq 1$  GeV is set at  $y_0 = 0.6$ , where small- $x$  quantum evolution becomes effective. The saturation scale for the dipole in the fundamental representation differs by a factor of  $Q_s^2 \rightarrow Q_s^2 C_F/C_A = \frac{4}{9} Q_s^2$ .

---

<sup>2</sup>Note that if hadron masses and intrinsic transverse momenta from fragmentation are neglected, then the rapidity of the produced hadron equals that of its parent parton. Hence, we do not distinguish between them.

$\gamma$  denotes the anomalous dimension of the target gluon distribution with saturation boundary condition and is modeled by KKT as

$$\gamma(y_h, q_t) = \frac{1}{2} \left( 1 + \frac{|\xi(y_h, q_t)|}{|\xi(y_h, q_t)| + \sqrt{2|\xi(y_h, q_t)|} + 7c\zeta(3)} \right). \quad (10)$$

Here, we have written  $\gamma$  as a function of transverse momentum rather than dipole size by evaluating it at a characteristic value  $r_t \sim 1/q_t$ . The free parameter  $c$  in (10) governs the onset of the quantum evolution regime, and has been fixed by KKT to  $c = 4$ .

The *Ansatz* (8) exhibits geometric scaling when  $\gamma$  is constant. Scaling violations are introduced into the KKT parameterization through the function

$$\xi(y_h, q_t) = \frac{\log(q_t^2/Q_0^2)}{(\lambda/2)(y_h - y_0)}. \quad (11)$$

$\xi$  vanishes as  $y_h \rightarrow \infty$  at fixed  $q_t$ , so that  $\gamma \rightarrow 1/2$ . On the other hand, approaching the saturation boundary at large rapidity far from the initial condition (i.e.  $q_t \rightarrow Q_s(y_h)$  for  $y_h \gg y_0$ ) leads to  $\xi \rightarrow 2$ . Due to the last term in the denominator of eq. (10) this corresponds to  $\gamma \approx 0.53$ , again close to the usual BFKL saddle point *without* saturation boundary conditions.

### 3 Scaling violations in the mid-rapidity RHIC data

It was shown in ref. [16] that the BRAHMS data [11] on forward hadron production from d+Au collisions at RHIC are described very well<sup>3</sup> by both the KKT [15] and the IIM [8] dipoles, provided that DGLAP evolution of the dilute projectile with exact splitting functions is taken into account. The predictions made in [16] appear to be confirmed by the preliminary data from STAR on  $\pi^0$  production at rapidity  $y_h \simeq 4$  [12]. The fact that both dipole parameterizations generically include an anomalous dimension of the target gluon distribution that *differs* from 1 at small  $x_A$  proved crucial. In particular, for  $y_h \gtrsim 3$  both KKT and IIM dipoles predict a nearly  $p_t$ -independent anomalous dimension  $\gamma \approx 0.6$  for  $p_t \lesssim 5$  GeV, which is close to the LO-BFKL prediction<sup>4</sup> of  $\gamma = \gamma_s \approx 0.627$  and, with eq. (1) from above, is consistent with the experimental  $p_t$  distributions [16].

In the present paper, we consider particle production in the central region,  $y_h = 0$ . As we shall see, here the behavior of  $\gamma$  required by the data and the CGC approach is very different. Before comparing to data, however, it is useful to analyze the kinematics. While forward hadron production probes rather small  $x_A$  in the target nucleus (c.f. appendix B in ref. [16]), one may wonder to what extent the conditions for applicability of the CGC formalism are met in the central rapidity region, for RHIC energy ( $\sqrt{s} = 200$  GeV). We

<sup>3</sup>Already at leading order in  $\alpha_s$ , if a phenomenological  $p_t$ -independent  $K$ -factor for NLO corrections is allowed for.

<sup>4</sup>This is the anomalous dimension for BFKL evolution with saturation boundary condition, i.e. for evolution along the saturation line.

expect that the CGC description breaks down beyond some  $x_0$ , where recoil effects affect the evolution with  $\log 1/x$ . Near  $x_0$ , knowledge of the *width*  $\Delta x/x_0$  of that transition region would also be required. Neither  $x_0$  nor  $\Delta x$  can be determined from the CGC formalism itself, since we presently lack a treatment of recoil and of other “large- $x$ ” effects within this approach.

However, since evolution in  $x$  appears to be quite rapid, it is probably not a bad approximation to consider a sharp boundary  $x_0$  beyond which the CGC small- $x$  formalism will break down. Experimentally, it is known that HERA data on proton structure functions at or below  $x_0 \sim 0.01$  can be described reasonably well within the small- $x$  evolution approximation [3, 4, 8, 9]. In case of nuclear targets, larger values of  $x_0$  are expected due to the  $\sim A^{1/3}$  enhancement of the saturation scale near  $x_0$  [20]. Therefore, for a rough estimate, we take  $x_0 = 0.05$  as the upper limit of validity of the small- $x$  approximation for the target.

At  $y_h = 0$ , the projectile and target  $x$  are equal and given by  $x = q_t/\sqrt{s}$ , with  $q_t$  the transverse momentum of the produced parton. If we assume that the small- $x$  approximation of the CGC can be applied for  $x < x_0 \simeq 0.05$ , then this translates into transverse momenta up to  $q_t \simeq 0.05\sqrt{s}$ . Thus, for RHIC energy the approach should be valid for  $q_t \lesssim 10$  GeV. Hadronization reduces this number by a factor of  $\approx 0.7$ , according to the typical values of  $z = x_F/x_p$  in the fragmentation. Hence, we estimate that in the central region the small- $x$  regime extends roughly up to hadron transverse momenta of  $p_t \simeq 7$  GeV.

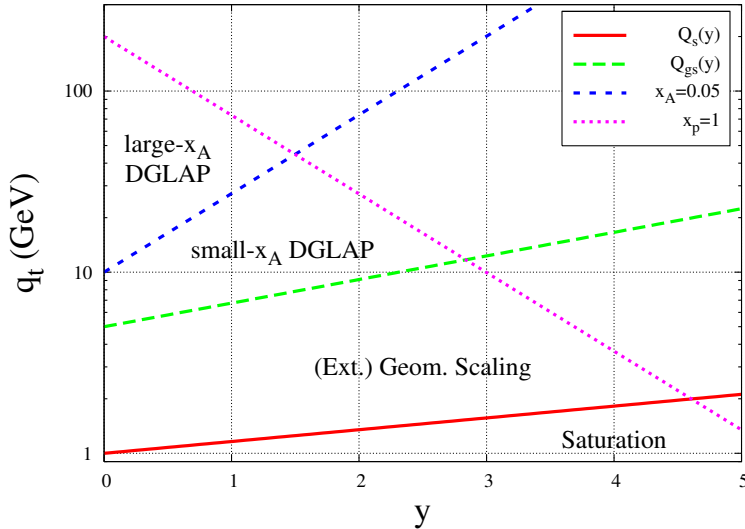


Figure 1: Schematic “phase diagram” of pA collisions at RHIC. For this plot, we have simply assumed that  $Q_s(y) = 1 \text{ GeV} \times \exp(\lambda y/2)$  and  $Q_{gs}(y) = Q_s^2(y)/200 \text{ MeV}$ ; see, however, sections 4 and 5.

This upper limit for the small- $x$  approximation is above the boundary between the extended scaling and the dilute DGLAP regimes,  $Q_{gs}(y) \sim Q_s^2(y)/\Lambda$  [7]. With  $Q_s^2 \simeq 1 \text{ GeV}^2$  at mid-rapidity (averaged over the transverse plane) and  $\Lambda = 200 \text{ MeV}$ , this

boundary occurs at a parton transverse momentum of about  $q_t \simeq 5$  GeV (or hadron transverse momentum  $p_t \simeq 3.5$  GeV). By this  $q_t$ , the anomalous dimension of the target gluon distribution should already have approached its DGLAP limit, starting from  $\gamma = \gamma_s$  at  $q_t = Q_s \simeq 1$  GeV. Hence, we expect large scaling violations in the central region of p+A collisions at RHIC already for transverse momenta on the order of a few GeV, signaling the approach towards the DGLAP regime. These different kinematical regimes are summarized in Figure 1. According to the discussion in the previous section, our approach via eq. (1) is valid up to  $q_t \simeq Q_{gs}$  but not much beyond.

These estimates are in qualitative agreement with the results of Accardi and Gyulassy [21]. They find that a resummation of the Glauber multiple-scattering series (which basically corresponds to semi-classical saturation) is required at  $p_t \sim 1$  GeV, and that a rapid transition to the DGLAP regime occurs towards higher transverse momenta. Comparing their approach to data from RHIC, they do not seem to find evidence for a broad geometric scaling window. In this vein, we also recall that a purely semi-classical model without quantum evolution does not reproduce the RHIC mid-rapidity data, as shown in [22]<sup>5</sup> (for an alternative approach, see [23]).

Similarly, leading-twist NLO pQCD [24] provides an accurate description of the mid-rapidity cross-section for  $p_t \gtrsim 5$  GeV. We point out that while this indeed contradicts the original GBW model, it is perfectly consistent with improved HERA fits including scaling violations [8] and with the CGC theory, which does predict that  $\gamma \rightarrow \sim 1$  for  $q_t > Q_{gs}$ . That this is perhaps the correct interpretation can be inferred from the *suppression* of scaling violations at large rapidity (and  $p_t \sim$  few GeV), which again is a generic prediction of the CGC approach<sup>6</sup>, and has already been verified to be consistent with RHIC data [16].

In Fig. 2 we show the transverse momentum spectra of charged hadrons at mid-rapidity for minimum-bias d+Au collisions at RHIC<sup>7</sup>. We also show the theory curves obtained from eq. (1), using CTEQ5-LO [26] parton distribution functions for the projectile deuteron, and KKP-LO [27] fragmentation functions at the scale  $Q_f = p_t$ . We plot curves for various *fixed* anomalous dimensions from  $\gamma = 0.5$  to 0.9. Clearly, a rather steep rise of the anomalous dimension in the  $p_t \sim 1 - 4$  GeV range is required for a satisfactory description of the mid-rapidity data. At the lower end,  $p_t \approx 1$  GeV, the anomalous dimension is close to 0.6, perhaps marking the onset of saturation dynamics in the weak-coupling regime. This observation is further supported by the fact that saturation based models successfully describe the hadron multiplicities at RHIC, which are dominated by soft hadrons [17]. On the other hand, at  $p_t = 4$  GeV, the anomalous dimension  $\gamma \approx 0.9$  required to fit the data nearly equals its leading twist DGLAP limit of 1.

To illustrate this further, we plot the transverse momentum dependence of  $\gamma$  for the KKT model in Fig. 3. For large transverse momenta, we assume that the Fourier transform of  $N_A(r_t)$  is dominated by transverse distances of order  $1/q_t \sim 1/(2p_t)$  and hence evaluate

<sup>5</sup>A fit is possible if one assumes an ad-hoc large “non-perturbative” contribution to  $Q_s$ , which has to be dropped again in the forward region. A critical discussion of this issue is given in ref. [22].

<sup>6</sup>Deriving from the fact that  $\Delta\gamma \sim 1/y$  at fixed  $p_t$ . See also refs. [25].

<sup>7</sup>For better visibility, we show only the BRAHMS [11] and STAR [13] measurements. Data at central rapidity has also been obtained by the PHENIX [14] collaboration.



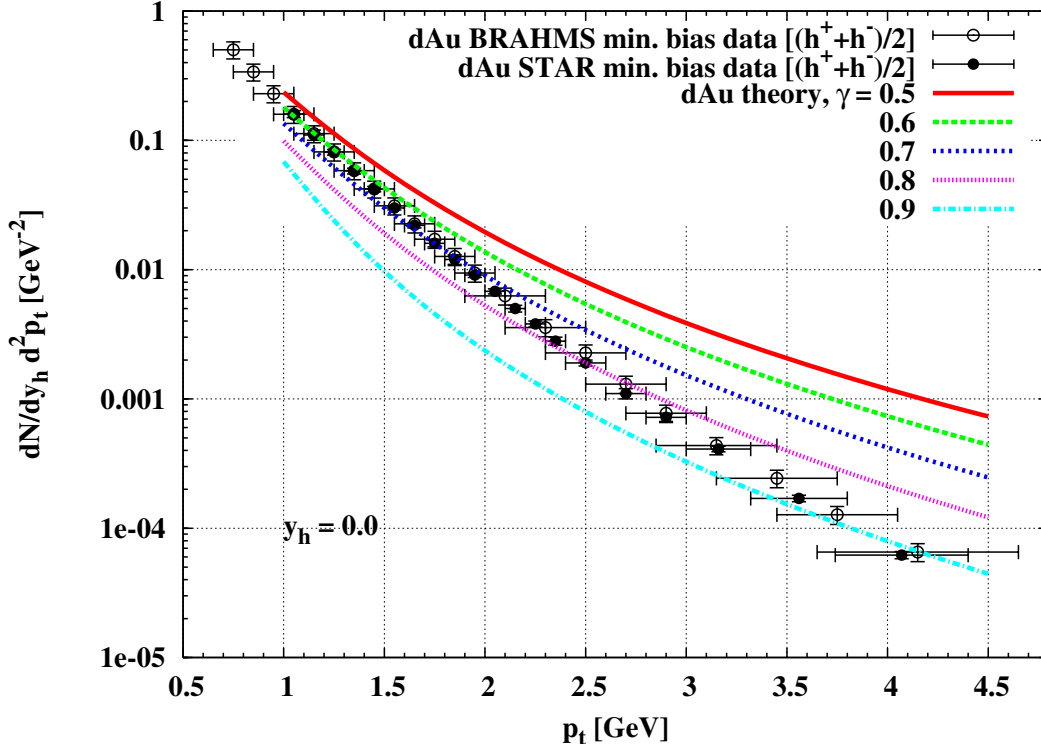


Figure 2: Charged hadron  $p_t$  spectrum obtained from eq. (1) using the KKT dipole for various fixed anomalous dimensions  $\gamma$ . The points with error bars show the BRAHMS [11] and STAR [13] data for minimum-bias d+Au collisions (RHIC, mid-rapidity).

$\gamma(r_t)$  at  $r_t = 1/(2p_t)$ .

One observes that the KKT parameterization of the anomalous dimension does not vary much with transverse momentum, staying within  $\approx 20\%$  of  $\gamma \approx 0.6$ . As discussed above, this behavior is generic to the CGC at *large rapidity* (i.e. small  $x_A$ ), and is consistent with the RHIC data [16]. However, we have also seen that the data requires a rapid approach towards the DGLAP regime at mid-rapidity and  $p_t \sim 4$  GeV, while  $\gamma_{KKT} \rightarrow 1$  only at asymptotically high  $p_t$ . In other words, we find evidence for substantial scaling violations at mid-rapidity, larger than those incorporated into the KKT parameterization but in agreement with our estimates on  $Q_{gs}$  from above, which then weaken at large rapidity (they get pushed to higher  $p_t$ ). Hence, the qualitative behavior of  $\gamma$  implied by the RHIC data is remarkably consistent both with HERA phenomenology and with the predictions of the CGC approach.

## 4 New parameterization of the anomalous dimension

Motivated by these results, we introduce a new parameterization of the dipole profile with an anomalous dimension incorporating stronger scaling violations, than the KKT dipole.

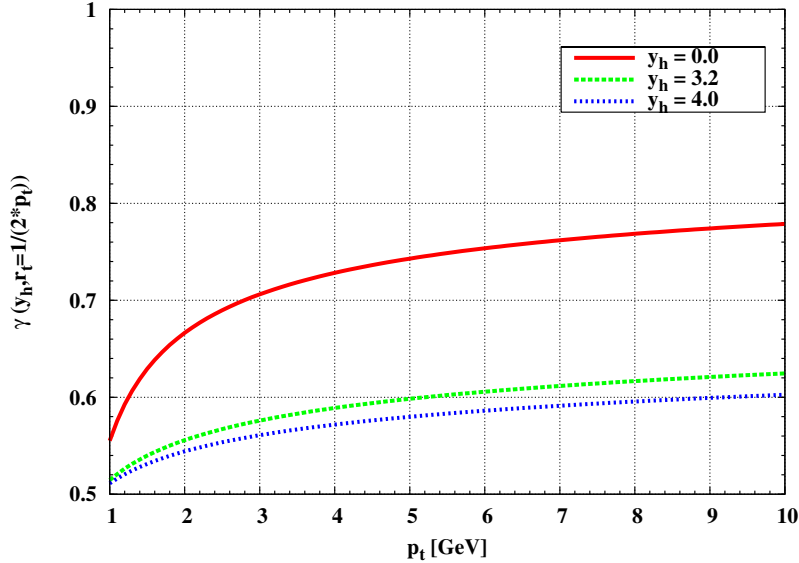


Figure 3: Anomalous dimension  $\gamma(y_h, r_t)$  of the small- $x$  nuclear gluon distribution for the KKT dipole model, evaluated at  $r_t = 1/(2p_t)$ .

At the same time, it corrects some deficiencies of the IIM dipole at large  $Q^2$ . In our parameterization, the anomalous dimension is given by

$$\begin{aligned} \gamma(Q^2, Y) &= \gamma_s + \Delta\gamma(Q^2, Y) \\ \Delta\gamma &= (1 - \gamma_s) \frac{\log(Q^2/Q_s^2)}{\lambda Y + \log(Q^2/Q_s^2) + d\sqrt{Y}}. \end{aligned} \quad (12)$$

We have written  $\gamma$  in terms of the variables appropriate for DIS, i.e.  $Q^2$  and  $Y = \log(1/x)$ , similar to the GBW and IIM models. Here,  $Q^2 \equiv 1/r_t^2$  is the *inverse transverse size of the dipole*, not to be confused with the factorization scale which enters the parton distribution and fragmentation functions in eq. (1). We shall transform into the variables appropriate for hadron-hadron collisions shortly.

The function is constructed such as to satisfy the following limits:

1. at any fixed rapidity  $Y$ ,  $\gamma \rightarrow 1$  for  $Q^2 \rightarrow \infty$ .
2. if  $Y \rightarrow \infty$  at fixed  $Q^2/Q_s^2(Y)$ ,  $\Delta\gamma$  decreases asymptotically like  $\sim 1/Y$ , as determined by BFKL [8]. This indicates that the geometric scaling window broadens with  $Y$ .
3.  $\gamma \rightarrow \gamma_s$  for  $Q^2 \rightarrow Q_s^2(Y)$  at any rapidity.
4. At large but fixed rapidity,  $Y \gg (d/\lambda)^2$ , the geometric scaling window reaches up to  $\log Q_{gs}^2(Y)/Q_s^2(Y) \sim \lambda Y$ , consistent with the asymptotic estimate for the geometric scaling window [7]:  $Q_{gs}^2 \sim Q_s^4/\Lambda_{QCD}^2$ .

This last condition is the most essential difference between our new parameterization and the IIM parameterization [8], where

$$\gamma_{IIM}(Q^2, Y) = \gamma_s + \frac{\log(Q^2/Q_s^2)}{\kappa \lambda Y}. \quad (13)$$

Here, one finds  $\log Q_{gs}^2/Q_s^2 \sim (1 - \gamma_s)\kappa\lambda Y$ , with  $\kappa \simeq 10$ . Hence, at large  $Y$ , their  $Q_{gs}^2(Y)$  is much larger than  $Q_s^4(Y)/\Lambda^2$ . Such behavior arises if the geometric scaling window is estimated from the diffusion term in the expansion of the LO-BFKL solution to second order about the saturation saddle-point. On the other hand, if  $Q_{gs}^2$  is estimated via the transition point between the LLA and DLA saddle points, respectively, one finds  $\log Q_{gs}^2/Q_s^2 \sim \lambda Y$ , without the additional factor of  $\kappa$  (for more details see, for example, section 2.4.3 in ref. [2] and references therein).

With  $\kappa\lambda Y$  replaced by  $\lambda Y$ , however,  $\Delta\gamma$  rises too rapidly with  $\log Q^2$  to allow for a good description of the RHIC data. Also, one should keep in mind that the IIM parameterization in fact provides a good fit to the HERA data on  $F_2(x, Q^2)$  at small  $x$ . Hence, strong modifications of  $\gamma$  are not desirable. As a consequence, to restore (approximate) agreement with the IIM parameterization, we are led to introduce terms which are subleading in  $Y$ . This agrees with indications from studies of small- $x$  evolution equations which show that at realistic energies (rapidities), subleading corrections to the asymptotic expressions are quite large. In (12), these are modeled by the  $\sqrt{Y}$  term with a free coefficient. From the mid-rapidity RHIC data, we extract  $d \simeq 1.2$  (see next section).

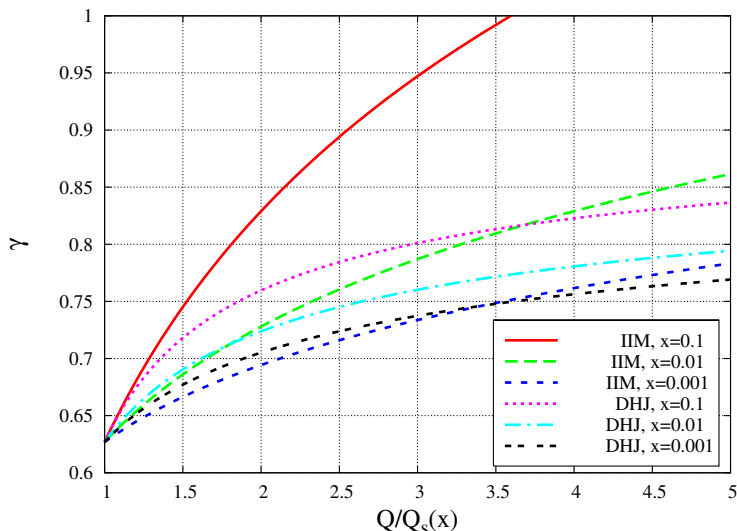


Figure 4: Anomalous dimension versus  $Q$  at various  $x$ .

Fig. 4 compares our dipole parameterization (12) with  $d = 1.2$  to that from eq. (13). At small  $x$  they are very similar as  $\gamma$  becomes flatter and approaches  $\gamma_s$ . Towards large  $x$ ,

$\gamma$  is somewhat smaller for our parameterization<sup>8</sup>. At the same time, the new anomalous dimension is closer to 1 than  $\gamma_{KKT}$ , which was shown in Fig. 3<sup>9</sup>, i.e. our parameterization features a narrower scaling window. With  $d = 1.2$ , which restores agreement with the IIM dipole at  $x = 10^{-3}$  and also describes the RHIC d+Au data correctly, the subleading term in the rapidity evolution of  $\gamma$  actually dominates until  $Y \simeq (d/\lambda)^2 = 16$ .

Finally, we also point to another recent parameterization of the dipole profile in ref. [22], which is meant to reproduce the RHIC data. That parameterization also includes breaking of geometric scaling at mid-rapidity, but not the sub-asymptotic terms for the evolution with rapidity. The dipole profile at large rapidity again resembles the KKT, IIM, and our present dipole model and so the forward hadron spectra “generated” by all these parameterizations should be rather similar.

## 5 Application to d+Au collisions at RHIC

For hadron-hadron collisions, we need to replace  $Q^2 \rightarrow 1/r_t^2$  and Fourier transform the dipole profile function from (8):

$$N_{A,F}(q_t) = \int d^2r_t e^{i\vec{q}_t \cdot \vec{r}_t} N_{A,F}(r_t) = 2\pi \int_0^\infty dr_t r_t J_0(r_t q_t) N_{A,F}(r_t). \quad (14)$$

Unfortunately, it is very challenging to perform this Fourier transform numerically when  $\gamma$  is not constant but  $r_t$ -dependent. It is therefore common to replace  $\gamma(r_t)$  by a constant  $\gamma(r_t = 1/q_t)$ , which makes the Fourier transform tractable [15, 16]. This is a reasonable approximation in the region where  $\gamma(r_t)$  is rather flat, e.g. at large rapidity and  $p_t \ll Q_{gs}$ . On the other hand, at mid-rapidity, where scaling violations are larger, we found that it is important to account for the  $r_t$ -dependence of the anomalous dimension, as this strongly affects  $N(q_t)$ .

However, with a  $r_t$ -dependent anomalous dimension, we were unable to perform the Fourier transform (14) numerically at very large transverse momentum, where the phase factor oscillates extremely rapidly. More importantly, the Fourier transform turns negative already at intermediate  $q_t$  ( $\approx 8$  GeV for gluons at mid-rapidity), where our numerical methods are still reliable. This unphysical behavior occurs for all of the above-mentioned  $\gamma(r_t)$  parameterizations (KKT, IIM and ours) and presumably indicates that the behavior of the function at very small  $r_t$  is inadequate<sup>10</sup>. We are nevertheless able to determine the transverse momentum spectrum of hadrons reliably up to about  $p_t = 4$  GeV, which doesn't receive contributions from the unphysical oscillations of  $N_A(q_t)$  at high parton momentum. As discussed in sec. 2, we do not expect that eq. (1) is valid much beyond this  $p_t$  at RHIC (mid-rapidity) anyways.

---

<sup>8</sup>Ref. [8] considered only the region  $x < 0.01$  and the fact that  $\gamma_{IIM}$  is not bounded from above was irrelevant for their analysis.

<sup>9</sup>Note also the factor of 2 difference in the  $p_t$ -scale at which  $\gamma$  is evaluated.

<sup>10</sup>This problem was encountered also in earlier studies [28] of Fourier transforms of the Bartels *et al.* DGLAP-improved dipole profile [3].

The field of the target nucleus is probed at the rapidity  $y_A$  given by  $y_A = \log 1/x_A = \log(1/x_p) + 2y_h$  (see appendix B in [16] for details of kinematic definitions). Hence, the saturation scale is defined at that rapidity,

$$Q_s^2(x_A) = Q_0^2 A_{\text{eff}}^{1/3} (x_0/x_A)^\lambda . \quad (15)$$

This implies that at fixed hadron rapidity  $y_h$ , as we sum the contributions from projectile partons with different momentum fractions  $x_p$  in eq. (1),  $Q_s(x_A)$  also varies.

The effective mass number of the nucleus depends on the impact parameter; following ref. [15], for heavy  $A \sim 200$  targets we do not perform the integral over  $b$  explicitly but take  $A_{\text{eff}} = 18.5$  for minimum bias collisions (the issue of impact parameter averaging is also discussed in ref. [22]). We fix the scale  $x_0 = 3 \cdot 10^{-4}$  to the value extracted in [3] by a fit to HERA data. With  $Q_0 = 1$  GeV, one obtains  $Q_s \simeq 1$  GeV at mid-rapidity for transverse momenta  $\sim 1$  GeV, which is reasonable [15].

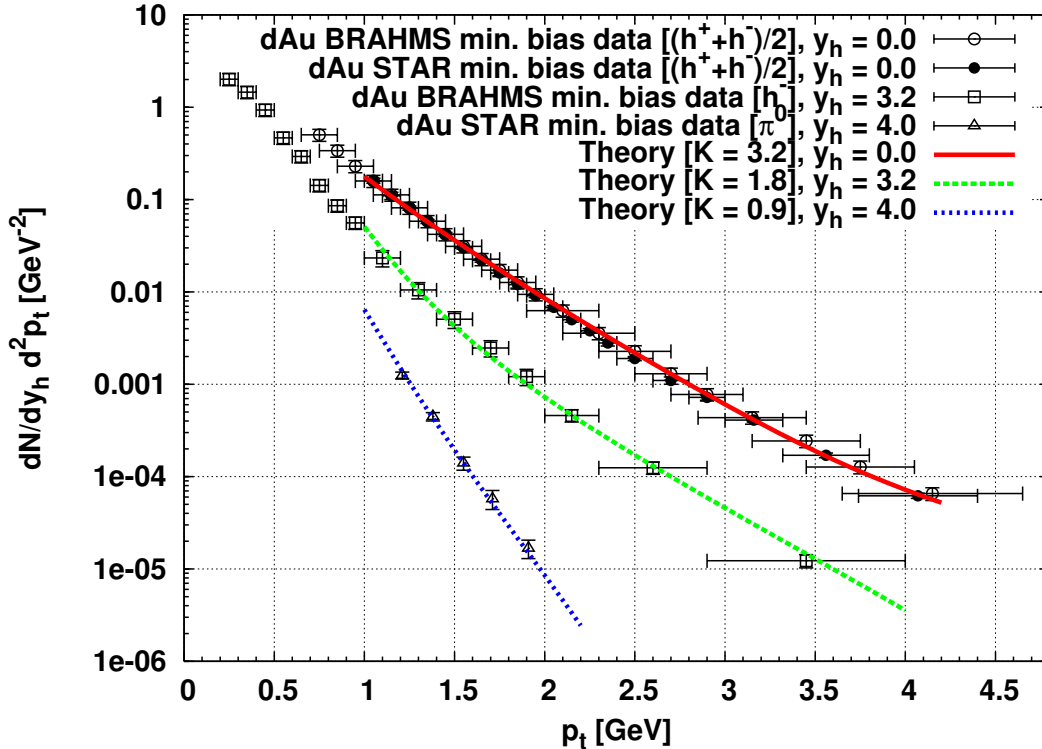


Figure 5: Comparison of theory and data [11, 12, 13] for minimum-bias d+Au collisions at RHIC energy.

In Fig. 5 we show our results for minimum-bias d+Au collisions at RHIC energy with the new parameterization (12). The factorization scale in eq. (1) is taken as  $Q_f = p_t$  for all rapidities. All other parameters have been fixed above. As promised, the shape of the mid-rapidity  $p_t$ -distribution is described quite well. For the correct overall normalization, we need to multiply our LO calculation by a factor  $K_{y=0} \simeq 3$ . This is much larger than at

forward rapidity, were  $K_{y=3} \simeq 2$  and  $K_{y=4} \simeq 1$ , respectively (for the same scale  $Q_f = p_t$  and the same parton distribution [26] and fragmentation [27] functions). Such a rapid increase of the  $K$ -factor towards mid-rapidity is expected because of larger phase space for NLO corrections<sup>11</sup>. Despite the good agreement of the LO curve with the  $p_t$ -dependence of the data, NLO calculations of particle production are clearly desirable.

Fig. 5 also shows that the new parameterization of the anomalous dimension introduced here describes the forward data as well as the IIM and KKT dipole models (for the latter, see curves in [16]). As already alluded to above, the reason for this generic behavior is that all models predict a rather flat  $\gamma(r_t) \approx \gamma_s$  at small  $x$  (wide geometric scaling window), and hence do not differ much. This also reflects in the fact that the forward rapidity curves from Fig. 5, which were obtained with the  $r_t$ -dependent anomalous dimension, are quite similar to those shown in ref. [16], which employed a constant  $\gamma = \gamma(r_t = 1/2p_t)$ . We stress that such good agreement with the data in the forward region is only achieved if the projectile parton distributions satisfy DGLAP evolution with *exact* rather than small- $x$  approximated splitting functions [16].

## 6 Summary

In summary, in this paper we extended our previous studies of forward rapidity hadron production in deuteron-gold collisions at RHIC to the central rapidity region. We argued that here the CGC predicts significantly larger scaling violations than at forward rapidity, and that indeed a relatively rapid transition of the anomalous dimension of the target gluon distribution from  $\gamma_s \approx 0.63$  (BFKL with saturation boundary conditions) to  $\gamma \rightarrow 1$  (DGLAP) is required by the data. It is important to note that this transition occurs in a regime where the small- $x$  approximation made in the Color Glass Condensate formalism is still valid. Hence, the scaling violations predicted by the CGC can indeed be tested.

We propose a new parameterization of the dipole profile which features a steeper transverse momentum dependence than the KKT dipole and leads to a satisfactory description of the mid-rapidity data. This agreement supports the predictions of the Color Glass Condensate formalism regarding the existence of different kinematic regions with different underlying physics.

Schematically, at small transverse momentum one probes the saturation region of the nucleus, where the underlying physics is that of a “black” target. As the transverse momentum increases, there is a transition from the saturation to the (extended) geometric scaling regime, corresponding to an anomalous dimension close to that from BFKL with saturation boundary condition. A further increase in the transverse momentum takes one beyond the geometric scaling region, signaled by the necessity of introducing rather large scaling breaking in the dipole profile. We showed that for transverse momenta of about 4 GeV, one is already in a small- $x$  DGLAP regime. Thus, the transition from the saturation to the DGLAP regions is quite narrow in the central rapidity region at RHIC. On the other hand, at large rapidity ( $y_h \gtrsim 3$ ) only the saturation and scaling regions remain, while

<sup>11</sup>This trend is also present in pQCD calculations of hadron spectra in proton-proton collisions [29].

the DGLAP window is cut off by finite-energy constraints, which has not been realized before. At LHC energy, all these kinematic regimes extend to even higher  $p_t$ , providing a great opportunity to study the various “phases” of high-energy QCD in more detail and with better accuracy.

## Acknowledgements

We would like to thank W. Vogelsang for helpful discussions. J.J-M. is supported in part by the U.S. Department of Energy under Grant No. DE-FG02-00ER41132.

## References

- [1] for recent reviews see, for example, A. H. Mueller, Nucl. Phys. A **715**, 20 (2003); E. Iancu and R. Venugopalan, hep-ph/0303204; L. McLerran, Nucl. Phys. A **752**, 355 (2005); E. Levin, J. Phys. Conf. Ser. **5**, 127 (2005) [arXiv:hep-ph/0408039].
- [2] J. Jalilian-Marian and Y. V. Kovchegov, Prog. Part. Nucl. Phys. **56**, 104 (2006).
- [3] K. Golec-Biernat and M. Wüsthoff, Phys. Rev. D **59**, 014017 (1999); Phys. Rev. D **60**, 114023 (1999); J. Bartels, K. Golec-Biernat and H. Kowalski, Phys. Rev. D **66**, 014001 (2002).
- [4] A. M. Stasto, K. Golec-Biernat and J. Kwiecinski, Phys. Rev. Lett. **86**, 596 (2001).
- [5] V. N. Gribov and L. N. Lipatov, Yad. Fiz. **15**, 781 (1972) [Sov. J. Nucl. Phys. **15**, 438 (1972)]; Yad. Fiz. **15**, 1218 (1972) [Sov. J. Nucl. Phys. **15**, 675 (1972)]; G. Altarelli and G. Parisi, Nucl. Phys. B **126**, 298 (1977); Yu. L. Dokshitzer, Sov. Phys. JETP **46**, 641 (1977) [Zh. Eksp. Teor. Fiz. **73**, 1216 (1977)]; Yu. L. Dokshitzer, D. Diakonov and S. I. Troian, Phys. Rept. **58**, 269 (1980).
- [6] E. A. Kuraev, L. N. Lipatov and V. S. Fadin, Sov. Phys. JETP **45**, 199 (1977) [Zh. Eksp. Teor. Fiz. **72**, 377 (1977)]; I. I. Balitsky and L. N. Lipatov, Sov. J. Nucl. Phys. **28**, 822 (1978) [Yad. Fiz. **28**, 1597 (1978)].
- [7] E. Iancu, K. Itakura and L. McLerran, Nucl. Phys. A **708**, 327 (2002); A. H. Mueller and D. N. Triantafyllopoulos, Nucl. Phys. B **640**, 331 (2002); E. Levin and K. Tuchin, Nucl. Phys. A **691**, 779 (2001).
- [8] E. Iancu, K. Itakura and S. Munier, Phys. Lett. B **590**, 199 (2004).
- [9] J. R. Forshaw and G. Shaw, JHEP **0412**, 052 (2004).
- [10] I. Balitsky, Nucl. Phys. B **463**, 99 (1996), Phys. Lett. B **518**, 235 (2001); J. Jalilian-Marian, A. Kovner, A. Leonidov and H. Weigert, Nucl. Phys. B **504**, 415 (1997), Phys. Rev. D **59**, 014014 (1999); E. Iancu, A. Leonidov and L. D. McLerran, Phys. Lett. B **510**, 133 (2001), Nucl. Phys. A **692**, 583 (2001); Y. V. Kovchegov, Phys. Rev. D **60**, 034008 (1999), Phys. Rev. D **61**, 074018 (2000).

- [11] I. Arsene *et al.* [BRAHMS Collaboration], Phys. Rev. Lett. **93**, 242303 (2004).
- [12] G. Rakness [STAR Collaboration], arXiv:hep-ex/0507093.
- [13] J. Adams *et al.* [STAR Collaboration], Phys. Rev. Lett. **91**, 072304 (2003); Phys. Rev. C **70**, 064907 (2004).
- [14] S. S. Adler *et al.* [PHENIX Collaboration], Phys. Rev. Lett. **91**, 072303 (2003).
- [15] D. Kharzeev, Y. V. Kovchegov and K. Tuchin, Phys. Lett. B **599**, 23 (2004).
- [16] A. Dumitru, A. Hayashigaki and J. Jalilian-Marian, Nucl. Phys. A **765**, 464 (2006).
- [17] for the general formalism see, for example, L. V. Gribov, E. M. Levin and M. G. Ryskin, Phys. Rept. **100**, 1 (1983); for applications to Au+Au and d+Au collisions at RHIC see D. Kharzeev and E. Levin, Phys. Lett. B **523**, 79 (2001); D. Kharzeev, E. Levin and M. Nardi, Nucl. Phys. A **730**, 448 (2004) [Erratum-ibid. A **743**, 329 (2004)]; for applications to p+p collisions at RHIC energy see M. Czech and A. Szczurek, Phys. Rev. C **72**, 015202 (2005).
- [18] D. Kharzeev, E. Levin and L. McLerran, Phys. Lett. B **561**, 93 (2003).
- [19] M. Ciafaloni, Nucl. Phys. B **296**, 49 (1988); S. Catani, F. Fiorani and G. Marchesini, Nucl. Phys. B **336**, 18 (1990); H. Jung and G. P. Salam, Eur. Phys. J. C **19**, 351 (2001); J. Kwiecinski, Acta Phys. Polon. B **33**, 1809 (2002); A. Gawron, J. Kwiecinski and W. Broniowski, Phys. Rev. D **68**, 054001 (2003).
- [20] L. McLerran and R. Venugopalan, Phys. Rev. D **49**, 2233 (1994); *ibid.* **49**, 3352 (1994); Y. V. Kovchegov, *ibid.* **54**, 5463 (1996); *ibid.* **55**, 5445 (1997); A. H. Mueller, Nucl. Phys. A **724**, 223 (2003); J. Jalilian-Marian, A. Kovner, L. D. McLerran and H. Weigert, Phys. Rev. D **55**, 5414 (1997).
- [21] A. Accardi and M. Gyulassy, Phys. Lett. B **586**, 244 (2004).
- [22] R. Baier, Y. Mehtar-Tani and D. Schiff, arXiv:hep-ph/0508026.
- [23] J. w. Qiu and I. Vitev, Phys. Lett. B **632**, 507 (2006).
- [24] V. Guzey, M. Strikman and W. Vogelsang, Phys. Lett. B **603**, 173 (2004).
- [25] D. Kharzeev, Y. V. Kovchegov and K. Tuchin, Phys. Rev. D **68**, 094013 (2003); J. L. Albacete, N. Armesto, A. Kovner, C. A. Salgado and U. A. Wiedemann, Phys. Rev. Lett. **92**, 082001 (2004); E. Iancu, K. Itakura and D. N. Triantafyllopoulos, Nucl. Phys. A **742**, 182 (2004).
- [26] H. L. Lai *et al.* [CTEQ Collaboration], Eur. Phys. J. C **12**, 375 (2000).
- [27] B. A. Kniehl, G. Kramer and B. Pötter, Nucl. Phys. B **582**, 514 (2000).
- [28] F. Gelis and J. Jalilian-Marian, unpublished.



- [29] K. J. Eskola, H. Honkanen, H. Niemi, P. V. Ruuskanen and S. S. Rasanen, Phys. Rev. C **72**, 044904 (2005); K. J. Eskola and H. Honkanen, Nucl. Phys. A **713**, 167 (2003).